Estimation of High-Precision Marine Geoid Models Offshore Newfoundland, Eastern Canada

G.S. Vergos✉
Department of Geodesy and Surveying, Aristotle University of Thessaloniki, University Box 440, 541 24, Thessaloniki, Greece, Fax: +30 31 0995948, email: vergos@topo.auth.gr

M.G. Sideris
Department of Geomatics Engineering, University of Calgary, 2500 University Drive N.W., Calgary Alberta, T2N 1N4, Canada

Abstract. The scope of this paper is to investigate the possibility of improving the determination of the marine geoid using heterogeneous data. To achieve this, altimetry, shipborne gravity, bathymetry and quasi-stationary sea surface topography (QSST) data are implemented in the modeling procedure using spectral methods. Special attention is paid to the modeling and removal of high-frequency oceanic phenomena contaminating the geodetic mission altimetry sea surface heights (SSHs) through local crossover adjustment and low-pass filtering. For validation purposes, comparisons with a regional gravimetric geoid model and Topex/POSEIDON (T/P) SSHs are performed, while the importance of crossover adjustment and low-pass filtering in removing part of the sea surface variability (SSV) is designated, especially for regions located is areas with high ocean dynamics. Furthermore, the results show that an altimetric geoid estimation accurate to about 7 cm (in terms of the standard deviation of the differences with T/P) is feasible, while the combination of altimetry and gravity data improves the gravimetric geoid determination by about 4-5 cm. Additionally, it becomes evident that special care is needed for altimetric gravity field modeling, while conclusions on the appropriateness of the proposed altimetric and gravimetric data processing algorithms are drawn in an effort to derive a unified approach.

Keywords. Marine geoid modeling, sea surface topography, sea surface variability, bathymetry.

1 Introduction

The estimation of a high-accuracy and high-resolution marine geoid model is of high importance, not only to geodesy but also to most Earth sciences. There exist numerous studies related to the use of altimetry data in marine gravity field modeling, all showing the great importance of implementing such datasets to improve the determination of the marine geoid (Andritsanos et al. 2001; Li and Sideris 1997; Vergos et al. 2001a). Most of these studies incorporate Fast Fourier Transform (FFT)-based methods and use the Input Output System Theory (IOST) for the optimal combination of heterogeneous, e.g., altimetric and shipborne gravimetric data (Sideris 1996; Vergos et al. 2001b). Their focus is more on the optimal combination of the input signals with respect to their heterogeneity rather than their optimal processing and treatment with the aim of a more accurate geoid determination. The focus of this paper is on the latter point, i.e. to derive optimal geoid models not only by combining heterogeneous datasets, but also by implementing additional information such as bathymetry and quasi-stationary sea surface topography (QSST) data in the processing procedures.

The effect of the ocean bathymetry in marine geoid modeling can be taken into account through regional or global Digital Depth Models (DDMs), in direct analogy to the Digital Terrain Models (DTMs) on land, using the various reduction methods such as the topographic reduction, the residual terrain modeling (RTM) reduction, and the isostatic reduction. Their use aims mainly at providing smoother residual fields prior to gridding, interpolation and/or prediction. According to Forsberg (1984), when high-quality depths are available, then the smoothing of the data can reach 50%.

The effect of the QSST is important in processing altimetry data since the SSHs available from the satellite do not refer to the geoid but to the sea surface, thus their processing will determine a very good model of the mean sea surface but not the geoid itself. Thus, it is important to correct the altimetry SSHs due to the presence of the stationary part of the SST by simply removing its contribution. Additionally, there are many cases that the available shipborne gravity data do not refer to the geoid but to the sea surface, i.e. the data are not free-air reduced. As in the case of the altimetry data, it is important to apply that reduction, using as height information the QSST, to refer them to the geoid.

Also, it is our aim to signal the importance of crossover adjustment and low-pass filtering in the reduction of oceanic effects contaminating GM altimeter data, especially in open ocean areas. It is well known that the effect of the SSV appears in the densely spaced GM SSHs as high-frequency noise, which should be reduced for a precise geoid determination.

2 Marine Geoid Modeling Methodology

Aiming at the determination of a precise marine geoid model for the area under study, purely altimetric, purely

gravimetric and combined solutions are computed. In the processing procedure, bathymetry as well as QSST data are implemented. Each of the three different solutions follows the remove-compute-restore scheme. The entire processing procedure is given explicitly for the altimetric geoid determination, while it is summarized for the gravimetric and combined ones.

2.1 Altimetric geoid modeling

Satellite altimetry data come in the form of SSHs that have to be corrected for the various geophysical effects and instrumental errors. After that step Corrected SSHs (CSSHs) are available from several satellites. Since for some (e.g. GEOSAT), observations refer not only to ocean but also land and shallow regions, a bathymetric mask has to be applied to remove the latter two. This is necessary since data over land and shallow regions contain in most cases errors, due to the scattering of the radar pulse by dry land and the shallow ocean floor and due to errors close to the coastline contained in the tide models used for the geophysical corrections.

A depth limit can be set arbitrarily so that measurements corresponding to depths greater than that will be rejected. A depth of -50 m was selected to leave the oceanic observations. In the authors' opinion, the selection of this depth value is area-dependant and its smallness does not play a significant role, since if it is too small then there will remain erroneous observations in the data, most of which can be removed with a simple 3 rms test in a later step. The so-derived SSHs refer to oceanic regions only and have to be reduced from the mean sea surface to the geoid by removing the contribution of the QSST. Most SST models come in terms of a spherical harmonic expansion of the dynamic ocean topography (DOT), so that the QSST can be computed for each SSH observation point as

$$\varsigma_c(\phi,\lambda)=\left[\sum_{n=1}^{n_{max}}\sum_{m=0}^{n}\left(\overline{C}_{nm}^{*SST}\cos m\lambda+\overline{S}_{nm}^{SST}\sin m\lambda\right)\overline{P}_{nm}(\sin\phi)\right] \quad (1)$$

where $\varsigma_c(\varphi,\lambda)$ is the contribution of the global DOT model coefficients, φ and λ denote the latitude and longitude, where the model's contribution is computed, n_{max} is the maximum degree of expansion, $\overline{P}_{nm}(\sin\phi)$ are the fully normalized associated Legendre functions and $\overline{C}_{nm}^{*SST}$, $\overline{S}_{nm}^{SST}$ are the fully normalized DOT spherical harmonic coefficients. It should be noted at this point that such global SST models are adequate for open ocean areas, but problematic for closed seas and close to the coast, where they should be used with caution.

The so-derived SSHs can be regarded as geoid heights and are thus processed to give the final geoid model using the remove-compute-restore method. Thus, the contribution of a geopotential model is removed to derive reduced SSHs. The so-referenced to a geopotential model SSHs may still contain some blunders, which should be removed, while the contribution of the bathymetry should also be taken into account. For the blunder detection, a simple 3 rms test is used, which is assumed to be sufficient to remove any erroneous data still present in the data. One of the considerations at this point is that for a 3 rms test to be applied, all biases in the dataset should be removed, so that only random errors remain. This will be decided by examining the mean value of the reduced SSHs. If the mean value is small enough, e.g. below 0.10 m, the 3 rms test is performed and then the altimetry SSHs are RTM-reduced to derive the final residual SSHs. On the other hand, if the mean value is higher, then it means that some biases are still present in the data and should be removed prior to the 3 rms test. This can be done by first RTM-reducing the SSHs, since when a good bathymetry model is used the resulting field is much smoother than the one prior to the reduction (Forsberg 1984).

The residual SSHs available at this point were derived as

$$N_{res}=N_{obs}-N^{GM}-QSST-N^{RTM} \quad (2)$$

where N_{obs} denotes the observed SSHs, N^{GM} is the contribution of the geopotential model and N^{RTM} is the effect of the bathymetry. The so derived SSH_{res} represent the medium wavelengths of the geoid height signal and can be safely regarded as residual geoid heights N_{res}. However, these measurements still contain the radial orbit error, due to the insufficient knowledge of the true satellite orbit, and the influence of time varying oceanic effects. It should be pointed out that due to the improved orbit modeling of the latest altimetric datasets, crossover adjustment may not be necessary for the reduction of the orbit errors, but may prove useful for the elimination of SSV-like effects (Knudsen 1992a, b). The statement about the reduction of the SSV is supported by the fact that the height differences that are adjusted at the crossover points contain neither the stationary geoid nor the QSST signals. Thus, with the exception of orbit errors, what mainly remains to be adjusted are: a) unmodeled tidal phenomena, b) the SSV and c) other dynamic ocean effects. Since the present study has a local character, a regional crossover adjustment scheme with one bias and one tilt parameter (Rummel 1993) is assumed sufficient.

After that step, the final geoid height estimates can be derived by first gridding the data. This is performed by using a weighted means with prediction power two type of gridding, taking into account the ten closest points for each grid node. Due to the small cross-track spacing of GM altimetric data (3-4 km for GEOSAT), SSV, especially in open ocean areas, may not be completely eliminated with crossover adjustment, and will still be present in the gridded N_{res}. Thus, as much as possible of that high-frequency information, considered as noise in the signal, should be removed before deriving the final altimetric geoid height estimates. This is achieved by low-pass filtering the gridded N_{res}, using a

collocation type of filter (Wiener filtering), assuming Kaula's rule for the geoid spectrum. If Kaula's rule is valid, then the power spectrum of geoid heights decays like q^{-4}, with q being the radial wavenumber. Following Forsberg (1984), the low-pass filter is

$$F(q) = q_c^4 / \left(q^4 + q_c^4\right) \quad (3)$$

where $q = \sqrt{u^2 + v^2}$, u and v denote radial wavenumbers and the cut-off frequency q_c is empirically determined based on maximum noise reduction with minimum signal loss (signal to noise ratio). In this filtering operation different cut-off frequencies should be tested to select the one that provides the best N_{res}, based on the aforementioned criterion. The final step to determine the altimetric geoid model is to restore the contribution of the geopotential model and that of the bathymetry. The procedure described in this section is given in Fig 1.

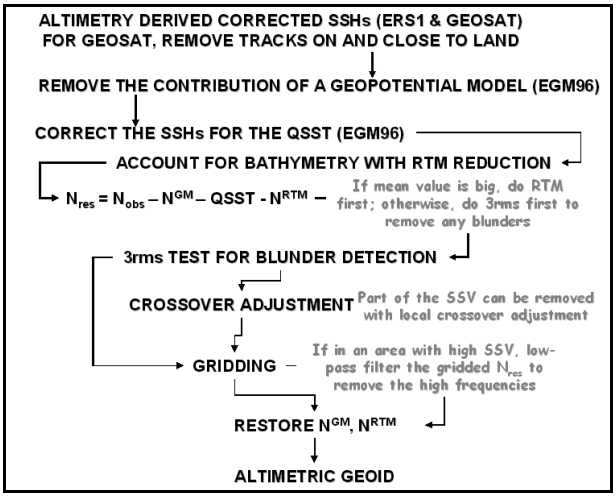

Fig. 1: Altimetric geoid modeling.

2.2 Gravimetric and combined geoid modeling

For the gravimetric and combined geoid modeling the aforementioned concept of the remove-compute-restore method is followed. The difference in the gravimetric geoid determination, w.r.t. the altimetric one, is in the handling of bathymetry. For the former one, the bathymetric reduction is applied once again in the remove step to smooth the residual gravity field, the residual gravity anomalies are then gridded and the contribution of the bathymetry is restored. Since the bathymetry refers to masses below the geoid, these have to be restored before the use of Stokes's formula. The direct bathymetric effect should not be confused with the use of the terrain correction in the solution of boundary value problems using Helmert's condensation method (Dahl and Forsberg 1998), where the primary indirect effect of the topography is restored after the prediction of the residual geoid field.

As far as the combined geoid modeling is concerned, the IOST has been implemented using the equations provided in Sideris (1996). The input signals were the two altimetric (ERS1 and GEOSAT) geoid models from sect. 2.1 and the gravimetric one. Since there was no available information about the input errors, randomly distributed noise fields (white noise) were generated. The variance of each field was based on the standard deviation (σ) of the difference of the respective geoid model with T/P SSHs. In the present study, the gravimetric geoid height prediction is performed using the 1D-FFT method and employing discrete spectra to evaluate Stokes' kernel function (Haagmans et al. 1993). No integration caps or modified kernels were used. The gravimetric geoid modeling methodology is described in Andritsanos et al. (2001) and will not be discussed here.

3 Data Used and Geoid Model Validation

The area under study is located offshore Newfoundland, Eastern Canada bounded between $40^o \le \varphi \le 50^o$ and $310^o \le \lambda \le 320^o$. ERS1 and GEOSAT GM as well as T/P altimetry data from the latest releases of their geophysical data records (GDRs) have been extracted for this area from the databases of NOAA (1997) and AVISO (1998), respectively. The gravimetric database was generated by shipborne gravity data available from Bureau Gravimétrique International (BGI) and the Geodetic Survey Division of Natural Resources Canada. Since their distribution was not sufficient in the eastern part of the region, they were augmented by the 2′×2′ KMS99 (Andersen and Knudsen 1998) multi-satellite altimetry-derived gravity field (Fig. 2). The local depth models used to take into account the effect of the bathymetry were those developed by Vergos and Sideris (2002) and Vergos (2002) using satellite altimetry and shipborne depth soundings. Finally, the EGM96 global geopotential model, complete to degree and order 360, and the EGM96 DOT, complete to degree and order 20, were used to provide the long wavelength geoid information and the QSST respectively (Lemoine et al. 1998).

For the validation of the estimated geoid models, stacked T/P SSHs, known for their high-accuracy, and the latest gravimetric geoid, CGG2000 (Véronneau 2001), of Canada were used. The complete dataset of T/P SSHs from the 3rd year of its mission was extracted so as to have more reliable results. In all cases the differences between T/P and the estimated geoid were computed and minimized using a four-parameter transformation model:

$$N^v = N^i - b_o \cos\phi\cos\lambda - b_1 \cos\phi\sin\lambda - b_2 \sin\phi - b_3 \quad (4)$$

where the parameters b_o, b_1, b_2 and b_3 were calculated by a least squares technique, N^v denotes the T/P SSHs or CGG2000 geoid used for the validation and N^i denotes the altimetric *(i=a)*, gravimetric *(i=g)* or combined *(i=c)* geoid height depending on the solution.

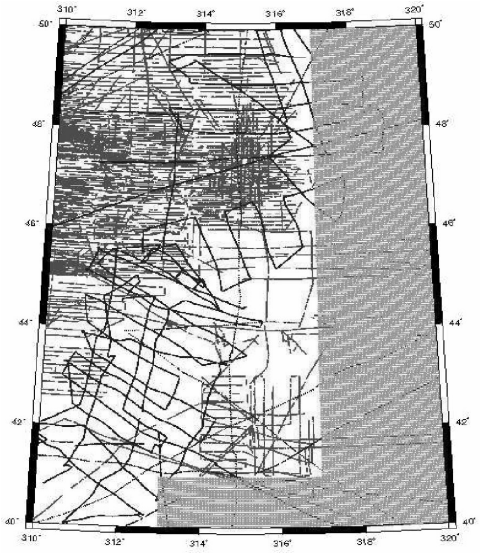

Fig. 2: Gravity data distribution (ship tracks: black, satellite altimetry: grey, Lambert projection).

4 Geoid Model Development

To derive the altimetric geoid models, 42640 and 76485 observations from the ERS1 and GEOSAT GM altimetry missions were used respectively. Local crossover adjustment of the satellite arcs was applied only for the case of GEOSAT, since the ERS1 data had been adjusted by AVISO. Table 1 shows the statistics of the GEOSAT residual geoid heights (N_{res}) and indicates that the field after the adjustment has a smaller σ by 3 cm compared to the one prior to crossover, while the mean value is also smaller by 1 cm. The estimated bias and tilt parameters are equal to 2.1 cm and -0.9 cm for the ascending arcs and -2.5 cm and 0.3 cm for the descending ones.

The small reduction of the mean value after the adjustment indicates that the new orbits of the altimetry data are determined very accurately so that crossover adjustment may not be necessary for the reduction of the radial orbit error, but for the elimination of other effects. Plotting the N_{res} before and after the adjustment some noisy characteristics in the central-eastern part of the area were identified and reduced after crossover. This area is known for its high ocean dynamics, since many currents and eddies are present, thus the high-frequency information contained in that region can be attributed to SSV. This is a good indication that crossover adjustment can reduce such effects in the densely spaced GM altimetry data.

Table 1. Statistics of GEOSAT N_{res} before and after the crossover adjustment. Unit: [m].

	max	min	mean	σ
before crossover	0.85	-0.84	0.13	±0.23
after crossover	1.19	-1.00	0.12	±0.20

After crossover adjustment, both the GEOSAT and ERS1 residual fields have been RTM reduced using the local bathymetry developed by Vergos (2002). Table 2 presents the statistics of the RTM-reduced N_{res} where a 3 rms test for blunder removal has also been applied. For GEOSAT, the blunder detection and removal was performed prior to the RTM-reduction, since the mean value was equal to -0.08 m only. For ERS1, the 3 rms test was performed after the RTM-reduction, since the mean value prior and after that was equal to 0.21 and 0.19 cm, respectively.

Table 2. Statistics of GEOSAT and ERS1 N_{res} before and after the RTM-reduction. Unit: [m].

	max	min	mean	σ
before (GEOSAT)	1.19	-1.00	0.12	±0.20
after (GEOSAT)	1.09	-0.98	0.10	±0.18
before (ERS1)	1.11	-0.99	0.21	±0.25
after (ERS1)	0.97	-0.95	0.19	±0.22

For both satellites, there is an improvement of both the mean and σ values after the RTM-reduction, as well as of the range of the N_{res}. These are reduced by about 2, 2 and 12 cm for GEOSAT and about 2, 3 and 18 cm for ERS1, respectively. These show that the resulting fields after the RTM reduction are indeed smoother. Another important point is that when a global DDM (JGP95E) was used, the residual fields became much rougher in both cases with the σ increasing to ±1.60 m for GEOSAT and ±1.65 m for ERS1 and the range to more than 7 m for both satellites, clearly due to errors included in that global DEM (Vergos and Sideris 2002). Thus, the use of DDMs in marine geoid modeling should be performed with caution, since an inaccurate and low-resolution model can degrade the results and lead to a less accurate estimation of the final geoid.

The final step is the filtering of the altimetry N_{res} to remove the high-frequency SSV effects which are especially evident in the eastern part of the area. The Wiener-type filter described in section 2 is used to low-pass filter the residual geoid heights, which are of course gridded prior to that step, on a 3′×3′ grid. Different cut-off frequencies are tested for both datasets and the optimal ones are selected based on maximum noise reduction with minimum signal loss. These are set to 6 km for GEOSAT and 8 km for ERS1. The selection of a shorter wavelength for the filtering of the GEOSAT data can be attributed partly to the elimination of part of the SSV in that dataset with crossover adjustment. For both satellites, the cut-off frequency is very close to the cross-track spacing of their sub-satellite points that is about 4-6 km for GEOSAT and 8-10 km for ERS1. Table 3 presents the statistics of the GEOSAT and ERS1 N_{res} after low-pass filtering. Comparing Table 2 (the last row for each satellite) and Table 3 it can be seen that the σ is reduced in both cases by about 2 cm, while the range of the residual fields is reduced as well by more than 35

cm. This is evident from Fig. 3 as well, where the GEOSAT N_{res} after filtering are presented since almost all noisy features in the eastern and southern part of the area, where the influence of the oceanic currents and that of the SSV seem to be especially significant, are greatly reduced.

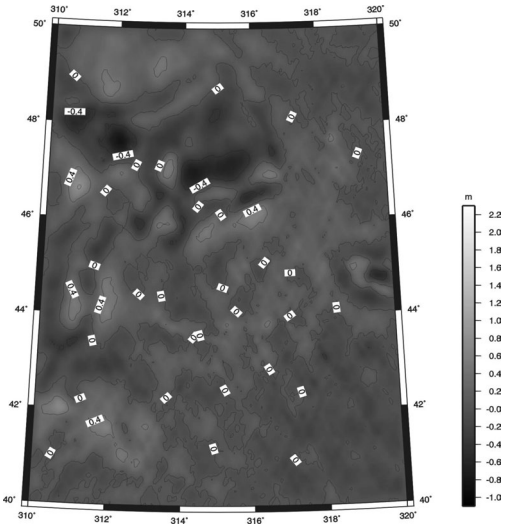

Fig. 3: GEOSAT-GM N_{res} after low-pass filtering.

Table 3. Statistics of GEOSAT and ERS1 N_{res} after filtering. Unit: [m].

	max	min	mean	σ
GEOSAT	0.82	-0.86	0.00	±0.18
ERS1	0.73	-0.90	0.00	±0.20

To derive the final altimetric geoid models, the contributions of the bathymetry and of the geopotential model were restored. The gravimetric and combined geoid solutions were derived based on the concepts presented in section 2. The statistics of these four solutions are summarized in Table 4.

Table 4. Statistics of the final altimetric, gravimetric and combined geoid solutions. Unit: [m].

	max	min	mean	σ
$\mathbf{N^{GEOSAT}}$	45.12	1.74	27.34	±8.81
$\mathbf{N^{ERS1}}$	45.05	1.66	27.24	±8.83
$\mathbf{N^{gr}}$	45.00	1.78	27.20	±8.83
$\mathbf{N^{comb}}$	44.90	1.77	27.24	±8.77

5 Validation of the Estimated Geoid Models

To assess the precision of the estimated models, comparisons with the latest gravimetric geoid model of Canada, CGG2000, and stacked T/P SSHs were carried out. Table 5 presents the comparisons between CGG2000 and the geoid models presented in this study. In all cases the differences were determined as N^{CGG200}-N^{i} where i represents the altimetric, gravimetric or combined geoid solutions. It is evident that the altimetric solutions agree with CGG2000, at the ± 20 cm level, and better, by about ±8 cm, compared to the gravimetric geoid. The combined solution shows an improvement compared to the gravimetric one at the 5 and 98 cm level, in terms of the σ and the range of the differences respectively. The noticing fact, in all comparisons, is the mean value of the differences, which is between -44 and -48 cm. Taking into account that the mean value of the EGM96 QSST used to reduce the data to the geoid surface is approximately 38cm, we can conclude that the effect of the stationary part of the SST was not taken into account in the development of CGG2000.

Table 5. Geoid height difference between CGG2000 and the estimated models. Unit: [m].

	max	min	mean	σ
$\mathbf{N^{CGG200} - N^{GEOSAT}}$	0.21	-1.33	-0.48	±0.21
$\mathbf{N^{CGG200} - N^{ERS1}}$	0.20	-1.25	-0.48	±0.20
$\mathbf{N^{CGG200} - N^{gr}}$	0.66	-2.06	-0.44	±0.28
$\mathbf{N^{CGG200} - N^{comb}}$	0.78	-1.22	-0.48	±0.23

Table 6 presents the geoid height differences between T/P SSHs and the estimated geoid models after the fit of a four-parameter transformation model. The same conclusions as in the previous comparisons hold, since the altimetric solutions present the smaller differences with T/P and the combined one gives an improved, compared to the gravimetric one, estimation of the geoid for the area. Worth mentioning though, is that the σ of the differences for the comparisons with the altimetric models is quite high, at the ±19 cm level, while a value close to ±9 cm would be expected based on previous studies (Andritsanos et al. 2001; Vergos et al. 2001a). Plotting the differences it was noticed that their largest values are located in the part of the region between $40^o \le \varphi \le 42^o$ and $310^o \le \lambda \le 316^o$ where the effects of SSV and other oceanic phenomena are very strong. In the rest of the region, the differences are within their expected values ranging between -40 and 50 cm. In our opinion, this is an indication that the accuracy of the altimetric geoid models is much better than the comparisons with T/P imply. Neglecting a few T/P points that refer to the aforementioned region the σ of the differences reduces to about ±5 to ±8 cm for the altimetric geoid models. The same improvement of more than ±9 cm holds for the gravimetric and combined models too. So, it can be concluded that by only stacking the T/P data part of the oceanic effects, which clearly influence the SSHs used for the comparisons, cannot be removed. Probably, the T/P data had to be low-pass filtered as well in their along-track direction, to further reduce the effect of the SSV and make the comparisons more representative.

6 Conclusions

Numerical investigations on marine geoid modeling using heterogeneous data have been presented aiming at the determination of high-accuracy geoid solutions and the derivation of an optimal data-processing scheme for related studies.

Table 6. Geoid height difference between T/P and the estimated models. Unit: [m].

	max	min	mean	σ
$N^{T/P} - N^{GEOSAT}$	0.63	-0.80	0.00	±0.19
$N^{T/P} - N^{ERS1}$	0.75	-0.76	0.00	±0.20
$N^{T/P} - N^{gr}$	0.92	-0.94	0.00	±0.28
$N^{T/P} - N^{comb}$	0.84	-0.93	0.00	±0.24

From the results and validation procedures carried out, it is evident that when altimetry and shipborne gravity data are handled properly, i.e. corrected for all error sources, blunders removed, accurate geopotential and DOT models used, the data are corrected for the QSST signal, the bathymetry is taken into account using an accurate model, the altimetry data are crossover adjusted and low-pass filtered, then, altimetric geoid modeling accurate to about ±7 cm is feasible, while the combined solution improves the gravimetric one, by about 4-5 cm, in terms of the σ of the differences with T/P SSHs.

The effect of oceanic phenomena in the densely spaced GM datasets, especially in areas with high ocean dynamics, is profound and should be reduced by crossover adjusting the altimeter datasets on a local scale as well as by low-pass filtering them. If this step is neglected, then the resulting geoid solutions are less accurate by about 2-5 cm.

The bathymetry should be taken into account only if an accurate model is available, whether else the geoid accuracy is reduced again. When local bathymetry models, validated and proven for their accuracy are not available, then the use of global DDMs, like JGP95E, should be implemented with caution, since they can lead to loss of accuracy. Finally, the altimetry data should be corrected for the QSST signal to refer to the geoid and not the sea surface, while the question that arises is not on the necessity of such a correction, but on the selection and the development of accurate DOT models.

Acknowledgements

This research was performed while the first author was a graduate student at the University of Calgary. Financial assistance, provided by NSERC and the GEOIDE Network of Centers of Excellence is gratefully acknowledged. Crossover adjustment, RTM reductions, griddind and filtering were performed using GRAVSOFT (Tscherning et al., 1993). BGI and Mr. Marc Véronneau from GSD/NRCan are gratefully acknowledged for providing the shipborne gravity data. We would like to thank the two reviewers, Will Featherstone and Marc Véronneau, for their constructive comments.

References

Andersen OB, Knudsen P (1998) Global gravity field from ERS1 and Geosat geodetic mission altimetry. J Geophys Res 103(C4): 8129-8137.

Andritsanos VD, Vergos GS, Tziavos IN, Pavlis EC, Mertikas SP (2001) A High-Resolution Geoid for the Establishment of the GAVDOS Multi-Satellite Calibration Site International Association of Geodesy Symposia, Vol 123, *Gravity, Geoid and Geodynamics 2000*, Sideris (ed.), Springer – Verlag Berlin Heidelberg, pp. 347-353.

AVISO User Handbook – Corrected Sea Surface Heights (CORSSHs). AVI-NT-011-311-CN, Edition 3.1, 1998.

Dahl OC, Forsberg R (1998) Geoid models around Sognefjord using depth data. J Geod 72: 547-556.

Forsberg R (1984) A study of terrain corrections, density anomalies and geophysical inversion methods in gravity field modeling. Report of the Dept. of geodetic Science and Surveying No 355. The Ohio State Univ., Columbus, Ohio.

Haagmans R, de Min E, van Gelderen M (1993) Fast evaluation of convolution integrals on the sphere using 1D FFT, and a comparison with existing methods for Stokes' integral. Manuscr. Geod. 18:227-241.

Knudsen P (1992a) Altimetry for Geodesy and Oceanography. In Geodesy and Geophysics, Kakkuri J (ed), pp. 87-129. Finnish Geodetic Institute.

Knudsen (1992b) Estimation of sea surface topography in the Norwegian sea using gravimetry and Geosat altimetry. Bull Géod 66:27-40.

Lemoine FG, Kenyon SC, Factor JK, Trimmer RG, Pavlis NK, Chinn DS, Cox C, Klosko SM, Luthcke SB, Torrence MH, Wang YM, Williamson RG, Pavlis EC, Rapp RH, Olson TR (1998) The development of the join NASA GSFC and NIMA geopotential model EGM96, NASA Technical Paper, 1998 – 206861.

Li J, Sideris MG (1997) Marine gravity and geoid determination by optimal combination of satellite altimetry and shipborne gravimetry data. J Geod 71(1): 209-216.

National Oceanographic and Atmospheric Administration – NOAA (1997) The GEOSAT-GM Altimeter JGM-3 GDRs.

Rummel R (1993) Principle of Satellite Altimetry and Elimination of Radial Orbit Errors. In Satellite Altimetry for Geodesy and Oceanography, editors: R. Rummel and F. Sansó, Lecture Notes in Earth Sciences No 50, pp. 189-241. Springer-Verlag.

Sideris MG (1996) On the use of heterogeneous noisy data in spectral gravity field modeling methods. J Geod 70(8): 470-479.

Tscherning CC, Forsberg R, Knudsen P (1993) The GRAVSOFT package for geoid determination. In: Holota P, Vermeer M (eds) 1st Continental Workshop on the Geoid in Europe, Prague, June 7-9, 1993, pp 327-334.

Vergos GS (2002) Sea Surface Topography, Bathymetry and Marine Gravity Field Modelling. MSc Theses Dissertation, Dept of Geomatics Engineering, University of Calgary, UCGE Reports 20157, Calgary, Alberta.

Vergos GS, Bayoud FA, Sideris MG, Tziavos IN (2001a) High-Resolution Geoid Computation by Combining Shipborne and Multi-Satellite Altimetry Data in the Eastern Mediterranean Sea. IGeS Bul Special Issue, Vol. 13, Proc of the EGS 2001 - G7 Session "Regional and Local Gravity Field Approximation", I.N. Tziavos and R. Barzaghi (eds.), pp. 85-99.

Vergos GS, Grebenitcharsky R, Sideris MG (2001b) Combination of Multi-Satellite Altimetry and Shipborne Gravity Data for Geoid Determination in a Coastal Region of Eastern Canada. IGeS Bul Special Issue, Vol. 13, Proc of the EGS 2001 - G7 Session "Regional and Local Gravity Field Approximation", I.N. Tziavos and R. Barzaghi (eds.), pp. 100-115.

Vergos GS, Sideris MG (2002) Improving the Estimation of Bottom Ocean Topography with Altimetry-Derived Gravity Data Using the Integrated Inverse Method. International Association of Geodesy Symposia, Vol. 124 Ádam J Schwarz KP (eds.), *Vistas for Geodesy in the New Millennium*, Springer – Verlag Berlin Heidelberg, pp. 529-534.

Véronneau M (2001) The Canadian Gravimetric Geoid Model of 2000 (CGG2000) Internal Report, Geodetic Survey Division, Natural Resources Canada, Ottawa.